Transmission of acoustic waves through mixing layers and 2D isotropic turbulence.

D. JUVÉ, P. BLANC-BENON and G. COMTE-BELLOT

Laboratoire de Mécanique des Fluides et d'Acoustique, URA CNRS 263
Ecole Centrale de Lyon, BP 163, 69131 ECULLY Cedex, France

Turbulence and Coherent Structures
O. Métais and M. Lesieur, eds.
Selected papers from "Turbulence 89: organized structures and turbulence in fluid mechanics"
Grenoble, 18-21 September 1989
© *Kluwer Academic Publishers, 1991*

Abstract

Ray tracing and parabolic equation methods have been used to study the properties of acoustic waves transmitted through turbulent velocity fields. A numerical simulation permits individual realizations of the turbulent field, which then allow, if desired, an ensemble averaging of the fields. Two flows have been considered, 2D isotropic turbulence, and a 2D mixing layer .The following complementary aspects are developed: the occurrence of caustics, the reinforced or weakened zones of the acoustic field, the eigenrays between a source and a receiver, and the associated travel times, variances, and scintillation index.

1. Introduction

The propagation of acoustic waves through inhomogeneous and/or random media has attracted a great deal of interest and its applications are numerous. Noise annoyance contours in the vicinity of industrial plants or airports have to include the pressure level changes due to the turbulence (wind or temperature) existing in the real atmospheric surroundings. In underwater acoustics, wave front distortions or phase changes have a direct effect on the detection ability of fixed or towed arrays used to locate noise sources. Remote sensing devices, such as sodars, used to detect high altitude turbulence as a complement to optical techniques, are based on the efficiency of the interaction between the acoustic waves and the flow. In all these cases there is a need for numerical models in order to estimate all the details of the interaction.

The classical method of handling the propagation of waves in random media relies on a statistical approach. As a first step, making use of several assumptions, one obtains an equation with random coefficients (Helmholtz or parabolic equation). Then other equations are deduced for second and higher moments (intensity, correlations...). The latter can only be closed using a hypothesis which implies, in essence, a very short correlation along the mean direction of the wave propagation (delta-correlated hypothesis). Initially this theory was developed for optical applications and the turbulent medium was characterized by a random refraction index. However, in acoustics, the presence of a flow introduces an additional effect of wave convection (ovalization of wave fronts) which is neglected in the classical approach.

We have developed a different approach in order to avoid purely statistical theory, not well-founded hypothesis, and inadaptation to fluctuating velocity fields. We use a deterministic propagation of an acoustic wave through numerically simulated turbulent fields. In this way not only one realization of the turbulent field can be created, but many and this allows for the obtaining of ensemble averages. Similar approaches were introduced very recently in optics (Martin and Flatte, 1988; Hesselink and Sturtevant, 1988). Our work presents several noteworthy differences : i) a consideration of velocity fluctuations instead of a refraction index such as in temperature changes (at least for part of the study) ; ii) a specifically tailored random field ; iii) simultaneous use of two complementary methods for describing acoustic waves (geometrical theory and the parabolic equation method).

In this article we will explain the non-averaged approach that we have developed and indicate its potentialities. We emphasize, in particular, the visualization of the acoustic field in order to illustrate the considerable deformation that it undergoes due to the cumulative effect of very weak turbulent fluctuations along the propagation path. These visualizations are presented, on the one hand for isotropic homogeneous turbulence and, on the other hand, for two steps of the downstream development of a 2 D mixing layer (Comte, Lesieur, Laroche and Normand, 1989). We also provide some quantitative statistical data in the case of isotropic homogeneous turbulence, not only in order to offer a comparison with existing theories, but also to demonstrate that new results can be generated.

Although the present work deals with two dimensional fields, its extension to three dimensional fields presents no essential difficulty if not a marked increase in calculating time. In fact 2 D and 3 D behaviors do not seem to be very different qualitatively (Blanc-Benon, Juvé, Karweit and Comte-Bellot, 1990) and this justifies our approach.

2. Modelling of acoustic wave propagation

The following two complementary descriptions are used : i) the geometrical acoustics approach which gives simple and clear visualizations of the focusing properties of a medium in random motion ; it is well suited to the computation of quantities linked to the transit time along the rays (wavefront distortion, phase fluctuations...) ; ii) The parabolic equation method which is well adapted to the determination of the energetics of the acoustic field (mean intensity, fluctuations, correlations...)

2.1. Geometrical acoustics

In this high frequency approximation, the acoustic variables, such as pressure $p(\vec{x}, t)$, are written in the form

$$p(\vec{x}, t) = A(\vec{x}).e^{iS(\vec{x})}.e^{-i\omega t}$$

where ω is the angular frequency. The amplitude A and the local wave vector $\vec{K}(\vec{x}) = \vec{\nabla}(S)$ are assumed to vary slowly on the scale of a wavelength $\lambda = 2\pi c_0/\omega$ (c_0 being the speed of sound). An asymptotic expansion for $\omega \to \infty$ of the exact linearized fluid mechanics equations gives the dispersion relation of acoustic waves propagating in an arbitrary velocity field $\vec{V}(\vec{x})$(Candel, 1977) :

$$\omega = Kc_0 + \vec{K}.\vec{V} \qquad K = \| \vec{K} \|$$

This non linear first order equation (for S) can be solved by the method of characteristics. The rays which are the lines tangent to the group velocity can be determined through the following Hamiltonian system :

$$\begin{aligned} \frac{dx_i}{dt} &= \frac{c_0 p_i}{p} + v_i \\ \frac{dp_i}{dt} &= -p_j \frac{\partial v_j}{\partial x_i} \\ p^2 &= (1 - \frac{\vec{v}.\vec{p}}{c_0})^2 \end{aligned}$$

where $\vec{p} = \vec{K}/k_0$ $(k_0 = \omega/c_0)$ is a non dimensional wave vector. The rays have been parametrized by the transit time from the source to a given point.

Plotting the rays permits a clear visualization of the trajectories followed by the acoustic energy radiating from an initially isotropic source. The spatial distribution of rays is a qualitative indicator of the local intensity of the field, since the square of the amplitude is inversely proportional to the cross-section of a ray tube. Quantitative information can be obtained by solving two additional differential equations (in 2 D) which govern the evolution along each ray of infinitesimal cross-section elements (Candel, 1977). It should be emphasized that the computation of acoustic intensity is, however, a difficult task at the crossing points of several rays. The amplitudes and travel times along each of these eigenrays have to be carefully determined in order to consider the multiple interferences existing at a given frequency. It is in fact more convenient to use a wave formulation such as the parabolic equation method which is described below. An important piece of information can be obtained from the evolution in space of an infinitesimal ray tube and that is the location of caustics (envelope of a family of rays) where the ray tube section vanishes. The geometrical approximation predicts infinite levels at the caustics (since diffraction is neglected) and, in practice, for high frequency waves this corresponds to a considerable reinforcement of the field. Prediction of the occurrence of caustics in random media is therefore an important research topic which has attracted a lot of theoretical work in recent years (White, 1984; Kulkarny and White, 1982).

2.2. The parabolic equation method

Unlike the geometrical approach, the parabolic equation method cannot be directly derived from the fluid mechanics equations in a linearized form. An "equivalent" inhomogeneous quiescent medium has to be defined and characterized by an index of refraction $n(\vec{x}) \simeq 1 - v_1(\vec{x})/c_0$ where v_1 is the component of the velocity field along the initial (unperturbed) propagation direction of the acoustic wave (Tatarski, 1971 ; Candel, 1979). This implicitly takes for granted that a "preferred " direction exists and that energy is scattered for the most part in a narrow conical region around this direction. Indeed this is the case when the ratio of the acoustic wavelength to the characteristic scale of the velocity field L is much smaller than one ($\lambda/L \ll 1$). When this condition is met, it is also possible to reduce the Helmholtz equation (which describes the propagation of waves in an inhomogeneous medium) to a parabolic form suitable for numerical treatment as well as for theoretical analysis (Tatarski,1971). Use of the envelope transformation $p(\vec{x}) = \Phi(\vec{x})e^{ik_0x}$, and suppression of the small term $\partial^2\Phi/\partial x^2$ gives :

$$2ik_0\frac{\partial\Phi}{\partial x} + \frac{\partial^2\Phi}{\partial y^2} + (n^2-1){k_0}^2\Phi = 0$$

This equation can be solved in an efficient way by using a spatial Fourier transform in the transverse direction. The field at abscissa $x+h$ is related to its value at x by the following algorithm (introduced in underwater acoustics by Tappert, 1977) :

$$\Phi(x+h,y) = e^{ik_0h(n^2-1)/2}\ \mathcal{F}^{-1}\ \{e^{is^2h/2k_0}\ \mathcal{F}\ \{\Phi(x,y)\}\}$$

Here, $\mathcal{F}$ denotes the direct Fourier Transform and s is the conjugate variable of y. The choice of the step h depends both on the wavelength and on the inhomogeneities of the medium (scales, fluctuation levels). In practice h can often be made to be much greater than λ rendering the algorithm very efficient (a detailed analysis of the errors inherent in this method can be found in DiNapoli and Deavenport,1979).

Two more questions remain to be solved : how do we choose the initial distribution of the pressure in the plane $x = 0$? and how do we suppress the artificial reflexions at the limits of the computation domain in the y direction ?

Our goal in the initialization of the field is to model a point source emitting in a limited angular sector ,typically $\pm 20°$ around the x-axis. This choice corresponds to our intention to compare the parabolic equation results with those of ray tracing. This spherical type of source is also closer to the ones used in experimental work than the plane wave frequently encountered in other numerical simulations. As shown by

Tappert (1977) a good initial field consists of a Gaussian distribution centered on the position of the source, its width being determined by the acoustic wavelength and the desired aperture angle.

The second question is solved by using a complex refraction index ; the small imaginary part induces a progressive artificial attenuation of the wave in the last 10% of the sampling points in the positive and negative y directions, so that the field is virtually reduced to zero at the two boundaries.

3. Propagation through 2D homogeneous isotropic turbulence

Most of the theoretical studies on wave propagation through random media have been developed for statistically isotropic and homogeneous fields. For these fields many results are available using various theoretical approaches such as geometrical acoustics, method of smooth perturbations, strong fluctuations theory, ... This offers opportunities to test our numerical scheme as well as some of the hypotheses used in theoretical studies.

3.1. Modelling of the random field

During the transit time of the acoustic wave the velocity field is, as usual, considered to be frozen. The medium can then be modelled by a sequence of independent realizations of a random field. Following Kraichnan (1970), the velocity at a given point $\vec{x}$ is simulated by the sum of a limited number N of random incompressible Fourier modes :

$$\vec{V}(\vec{x}) = \sum_{l=1}^{N} \vec{U}(\vec{K}^l) \cos(\vec{K}^l.\vec{x} + \Psi^l)$$

$$\vec{U}(\vec{K}^l).\vec{K}^l = 0$$

The direction of the wave vector $\vec{K}^l$ and the phase Ψ^l are independant random variables with uniform distributions. In our simulations, we have considered the amplitude $\| \vec{U}(\vec{K}^l) \|$ to be a deterministic variable whose value is set according to the energy spectrum $E(K)$ under consideration. In this paper we have used a field with a Gaussian correlation function $f(r) = e^{-r^2/L^2}$, where L is related to the integral scale L_f by $L_f = L\sqrt{\pi}/2$. This form is often encountered in theoretical investigations due to its analytical simplicity. It is also convenient for numerical simulations because it covers a limited range of energetic wave numbers. In 2D the energy spectrum is related to f(r) by the general formula :

$$E(K) = \frac{v'^2}{2} K \int_0^\infty \frac{\partial}{\partial r}(r^2 f(r)) \, J_0(Kr) dr$$

J_0 is the Bessel function of the first kind of zero order and v'^2 is the mean square value of the velocity fluctuations. With the Gaussian correlation function $f(r)$ indicated above one obtains :

$$E(K) = v'^2 \frac{K^3 L^4}{8} \ e^{-K^2 L^2/4}$$

In our simulations this spectrum has been sampled with $N = 50$ modes linearly distributed between $K_{min} = 0,1/L$ and $K_{max} = 10/L$. In order that the mean properties of the simulated field be close to the desired ones (homogeneity, isotropy, correlation length), the minimum number of realizations of the field has to be around 500 (Blanc-Benon *et al.*, 1990). For acoustic quantities, however, the global trends are obtained with only 100 realizations, because of a further mean along the propagation path.

It is important to note that the description in terms of Fourier modes presents a definite advantage for ray tracing : the differential equations to be solved contain first order (geometry of rays) and second order (ray tube cross-sections) derivatives of the velocity field. In our simulation these derivatives are obtained analytically, avoiding the usual finite-difference approximations. Numerical errors are then reduced and computation time is saved.

3.2. Acoustic field visualizations

The first figures provided illustrate the large distortions that acoustic waves undergo when travelling through one realization of a turbulent velocity field even though the fluctuation rate is weak (turbulent Mach number$M_t = v'/c_0$ less than 0.01). These visualizations also present an additional interest, which is to allow at least a qualitative confrontation between the two approaches used. The obtaining of figures with similar tendancies is a proof of the validity of our results, since each of the approaches is based on different approximations : high frequencies for geometrical acoustics ; definition of an equivalent refraction index for the parabolic method.

In geometric acoustics the only characteristic length scale is the parameter L introduced in the correlation function $f(r)$. The various visualizations are therefore presented in non dimensional variables x/L and y/L . The turbulent Mach number is equal to 6.10^{-3}. The maximum propagation distances are $x/L = 30$ and $x/L = 60$. For the parabolic approximation, three values of λ/L were retained : $\lambda/L = 0.05; 0.01; 0.2$. The source emission is within an angle of $\pm 20°$ in respect to the x-axis. These values have been selected according to two criteria : on the one hand, it is necessary to respect the application conditions of the theories ($\lambda/L \ll 1$, small angles, weak fluctuations) ; on the other hand,

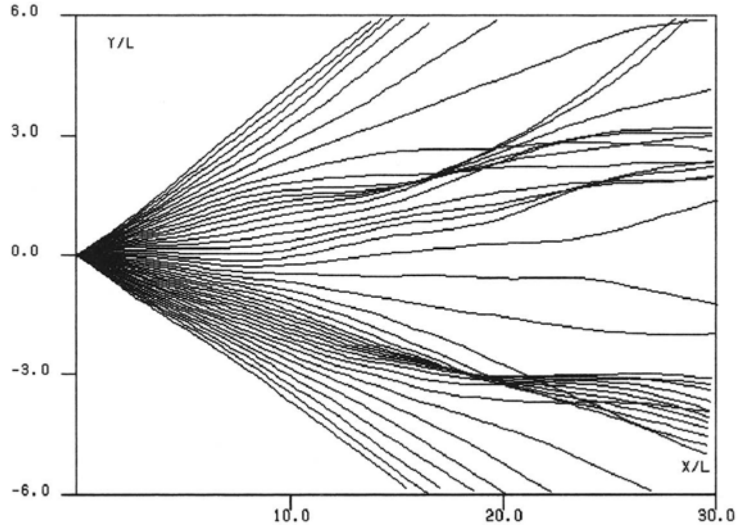

Fig.1. Propagation of acoustic rays in a single realization of a 2D isotropic velocity field ($v_1'/c_0 = 0.003$, $L = 0.1m$). ote the distortion of rays and the occurrence of caustics

the observed effects should correspond to realistic situations (in spite of the 2D character of the modelisation) such as those found during propagation in the atmosphere or in laboratory experiments simulating it (Blanc-Benon and Juvé 1987).

Figure 1 shows a typical example of ray tracing through a turbulent field realization. It can be noted that the initially linear trajectories launched at regularly spaced angular intervals ($\Delta\theta = 0.5°$) are highly deformed. When two neighboring rays are observed, large increases or decreases of the cross-section of elementary tubes can be seen. Accordingly, large local variations of the acoustic intensity are obtained and have to be connected to the occurrence of caustics as soon as a sufficient distance from the source is reached. In Figure 1, two strong concentrations of rays occurred around $\theta = -9°$ and $x/L = 20$ and around $\theta = 5°$ and $x/L = 15$; a third weaker caustic occurs around $\theta = 3°$ and $x/L = 25$.

Figure 2 (see colour plates) corresponds to the same realization but depicts a distribution of acoustic levels using the parabolic equation method with $\lambda/L = 0.1$. In order to eliminate the geometrical spreading of the wave, we expressed the results in terms of a ratio of the acoustic intensity obtained with turbulence to the acoustic intensity in a homogeneous medium. This ratio was then expressed in color levels according to a logarithmic scale . The dark red, for example, corresponds to a reinforcement of the initial level equal to or above 10 dB, which is highly significant. The similar behavior of this figure and Figure 1 is striking. In particular, the high increase zones of the level directly correspond to the caustics predicted by the geometrical theory. The decrease zones of the level are between caustics and associated with regions where few rays pass. It is also interesting to observe the elongated filament structure in the direction of local propagation. This structure corresponds to an aforementioned suggestion that, for $\lambda/L \ll 1$, scattering mostly occurs within small angles. As a result, the field evolution is much more gradual in the axial direction than in the transverse one, thus permitting a rather large step. For Figure 2 we chose $\Delta x/L = 0.1$ (i.e. $\Delta x = \lambda$ and $\Delta y/L = 0.025$) which are rather conservative values.

Figure 3 (see colour plates) depicts the effect of a wave frequency multiplied by 2 (that is $\lambda/L = 0.05$) for the same turbulent field realization. All the characteristic traits of Figure 2 are found, but this time with a greater sharpness of details especially perceptible in the transverse direction. This result corresponds to the decrease of the low frequency filtering effect : in the acoustic field (not too close to the source) no detail less than the wavelength can be detected. The wave frequency effect is therefore relatively modest. The effect of the characteristic length scale L of the turbulent field is much larger as seen in Figure 4 (see colour plates) where L is half the size of that in Figure 2 (with $\lambda/L = 0.2$). The spatial evolution of the intensity is clearly more rapid than previously. This can bee seen for example in the region of weak intensity around the x-axis. These evolutions correspond rather well to the idea according to which the characteristic length scale of the axial variation of intensity fluctuation would be k_0L^2 or L^2/λ, showing a greater sensitivity to a modification of L rather than to a modification of λ (Spivack and Uscinski, 1988).

3.3. Some additional results

The following results deal with average acoustic field properties obtained using both the ray and the parabolic equation methods. As a whole, these results are in agreement with theoretical prevision ; this validates our simulation technique. However, in certain cases, the theory and the simulation separate and it would seem that the differences noted are due to a deficiency of certain assumptions of theoretical developments. The latter constitutes a justification for using the deterministic approach.

i) Travel time along the rays

One of the most interesting parameters that the geometric theory can provide is the travel time between a source and a receiver in an effort to reconstruct wave fronts perturbed by turbulence. Fluctuations in this travel time were studied theoretically as early as the 1960's by Chernov

(1960) and Keller (1962). The essential result deals with the variance of the travel time fluctuation which is expressed by the following formula:

$$\overline{\Delta t^2} = \frac{2\mu^2}{{c_0}^2}\, l_c\, x$$

where $\mu = v_1'/c_0$, l_c is the correlation length scale of the random field, x the distance between the source and the receiver.

In Figure 5 we show the variances obtained for two values of the rms velocity fluctuation ($v_1'/c_0 = 0.003; 0.006$). For the weaker value, the agreement between theory and simulation is very good: the evolution of $\overline{\Delta t^2}$ with x is in particular very linear up to around $x/L = 30$; the simulated variance increases afterwards slightly more quickly than predicted. For the second rms value, the difference between theory and simulation rapidly increases. The linear increase of $\overline{\Delta t^2}$ with x occurs only up to $x/L = 15$; afterwards $\overline{\Delta t^2}$ exhibits an almost quadratic growth, with a simulated value at $x/L = 40$ which is twice as big as that predicted by the Chernov theory. The reason for this behavior is not yet entirely clear, but it would seem to be directly linked to the existence of caustics. The higher the turbulent intensity, the shorter the distances at which the first custic occurs. The focalisation effect therefore becomes essential. As long as no caustic occurs, only one eigenray links the source to the receiver. If one caustic occurs, three eigen-rays coexist with different travel times and, qualitatively, this can lead to an increase in the variance of real travel times in relation to the theoretical predictions which implicitly assume the existence of a unique eigenray. To consolidate this point of view, Codona and al (1985) have recently demonstrated the importance of the occurrence of caustics when evaluating the average travel time in a random scalar field.

The probability of the appearance of the caustics in a random scalar field has recently been theoretically explored by Kulkarny and White (1982). In our numerical simulation applied to the evolution of the cross section of an elementary ray tube, we determined the point at which a given ray touches a caustic and then we estimated the probability density of occurrence of the first caustic (Blanc-Benon and Juvé, 1990). In Figure 6 we report the results obtained for the two values of the r.m.s. velocity fluctuation. The curves present the shapes predicted by Kulkarny and White (1982). The probability of meeting a caustic is very small up to a certain distance. Afterwards the probability increases rapidly, reaching a maximum before slowly decreasing in a quasi exponential way. However, the probability density maximum which should theoretically occur at $s = 3.5$ according to Kulkarny and White (1982) occurs instead at 2 (s is defined as $s = 12^{1/3}\pi^{1/6}\mu^{2/3}\ x/L$). This difference can no doubt be explained by the vectorial character of our random velocity

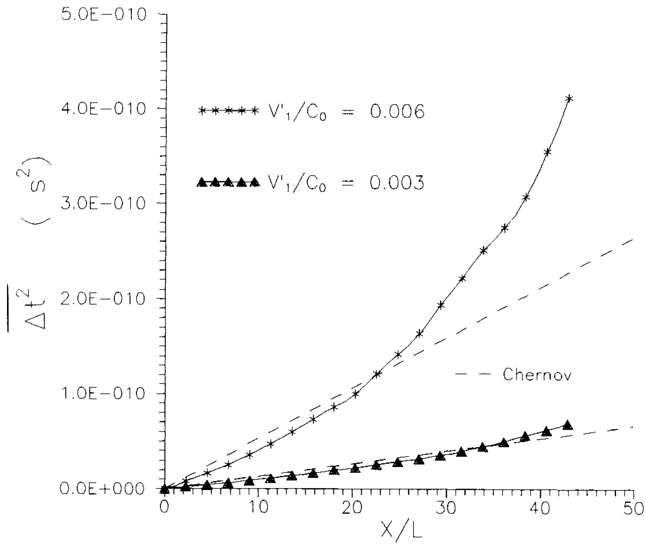

Fig.5. Variances of arrival time on a circle of radius x from an acoustic point source (2D isotropic field, $v_1'/c_0 = 0.003$ and 0.006, L = 0.1 m ; 250 realizations). Continuous curves are Chernov predictions

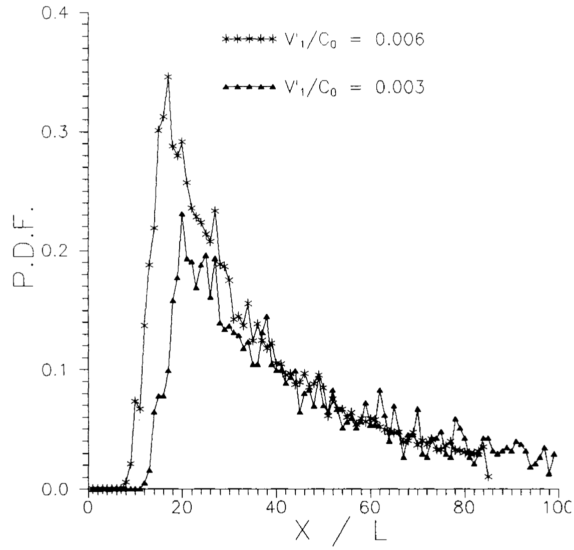

Fig.6. Probability density function for the occurrence of the first caustic (2D isotropic field, $v_1'/c_0 = 0.003$ and0.006, L = 0.1 m ; 250 realizations)

field. For the same characteristic length scale L introduced in the correlation function f(r), the kinetic energy spectrum is richer in spatial high frequencies than in the scalar case studied by Kulkarny and White (1982). The existence of these more energetic small structures leads to a wave focalisation at a shorter distance, which is precisely what is seen in the simulations. In addition, we note that the maximum of the probability distribution is obtained at $x/L = 32$ when $v_1'/c_0 = 0.003$ and earlier at $x/L = 20$ when $v_1'/c_0 = 0.006$ and that, at the same respective distances, the variances obtained by simulation begin to slightly differ from the theoretical predictions.

ii) Intensity fluctuations

To obtain quantitive information on the acoustic intensity at a given point is difficult in geometrical acoustics. On the contrary, the parabolic equation method is ideally suited for this. The most significant parameter of intensity fluctuation is the standard deviation $\sigma_I = \sqrt{\left\langle (I - <I>)^2 \right\rangle / <I>^2}$ (in optics σ_I^2 is known as the scintillation index). In the domain of small fluctuations the Rytov approximation gives results for the log amplitude fluctuations $\chi = \ln(A/A_0)$; A_0 is the field amplitude in the absence of perturbation, and the standard deviation σ_χ is approximately linked to $(\sigma_I)_{Rytov}$ by $(\sigma_I)_{Rytov} = 2\sigma_\chi$. In the case of a spherical wave in a Gaussian random medium, $(\sigma_I)_{Rytov}$ is then found by Ishimaru (1978) to be :

$$(\sigma_I)^2_{Rytov} = 2\sqrt{\pi} \left(\frac{v_1'}{c_0} \right)^2 Lk_0{}^2 \int_0^x 1 \Big/ \left(1 + \frac{k_0^2 L^4 x^2}{16\eta^2 (x-\eta)^2} \right) d\eta$$

A saturation phenomenon is also known to occur in the scintillation index for values of σ_I close to 1 . This behavior has been experimentally observed and predicted by ad hoc asymptotic theories (Tatarski, 1971 ; Tatarski and Zavorotnyi ,1980) which even indicate a slight decrease of the standard deviation for $(\sigma_I)_{Rytov} \gg 1$. No theory currently exists to predict behavior in the transitional region between the Rytov calculation and the asymptotic expression mentionned above. It is in this region, which is perhaps the most interesting, at least in acoustics, that our numerical simulation furnishes the most new elements.

Our results on that topic are presented in Figure 7.

Two frequency and two scale L values are used (corresponding to $\lambda/L = 0.05; 0.1; 0.2$ when $v_1'/c_0 = 0.006$). In these situations the strength parameter $\Gamma = k_0^3 \mu^2 x^2 l_c$ defined by Spivack and Uscinski(1988) ranges from around 2 to 120. In the weak fluctuation region (σ_I less than around 0.3 to 0.5) the agreement with the Rytov formula is excellent. The computations then show the transition towards a σ_I plateau culminating slightly above 1 and depending on Γ . However, it is not possible

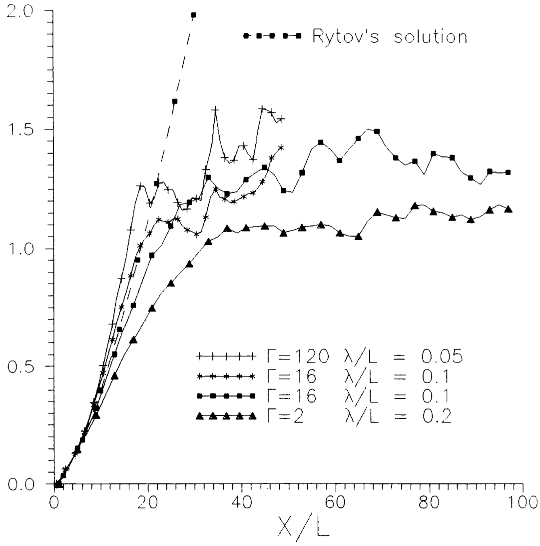

Fig.7. Standard deviation of acoustic intensity fluctuation (2D isotropic field, $v_1'/c_0 = 0.003$ and0.006, L =0.1 m; $\lambda/L = 0.05, 0.1, 0.2$; 250 realizations)

to detect any decrease tendancy whatever for σ_I. It must nevertheless be noted that, at a great distance, the acoustic level is strongly reduced due to the beam divergence, and moreover, a greater number of realizations would be required to reduce the residual curve oscillations. Finally, let us also add that Spivack and Uscinski(1988), using a different approach and an equation governing the 4th order moment, also obtained a plateau for σ_I, after a maximum whose position and height depend on the strength parameter.

4. Propagation through a 2D mixing layer

The mixing layer which has been the subject of numerous investigations, both experimental and numerical, is also of great interest to our study. Its principal characteristic is the formation of vortices which can coalesce (Corcos and Sherman, 1984; Lesieur *et al.*, 1988). We have chosen to show the influence of such a flow on the propagation of acoustic waves emitted perpendicular to the mean flow direction. A possible application could be the use of the modulation of the transmitted acoustic beam as a means to detect the existence of well-defined turbulence structures. The most interesting stage of the merging of two structures has been retained. Two computations were carried out, immediately before and immediately after the coalescence. The velocity fields corresponding to these two time steps were graciously furnished by P. Comte from the Fluid Mechanics Laboratory in Grenoble (Comte *et al.*, 1989). His computations were made for a 2D mixing layer increasing in time. The initial field has a stream function $\Psi = U\delta_0 \log(cosh(y/\delta_0))$, the vorticity thickness is given as $\delta_i = 2\delta_0$. The computation domain is square, with a side equal to four times the most amplified wave length predicted by the inviscid linear stability theory ($\lambda_{st} = 7\delta_i$) . The initial Reynolds number based on δ_i and U, the half velocity difference, is 1000. Accordingly, our acoustic wavelength λ was chosen in such a way that $\lambda \sim .2\delta_i$, the Mach number U/c_0 being 0.03.

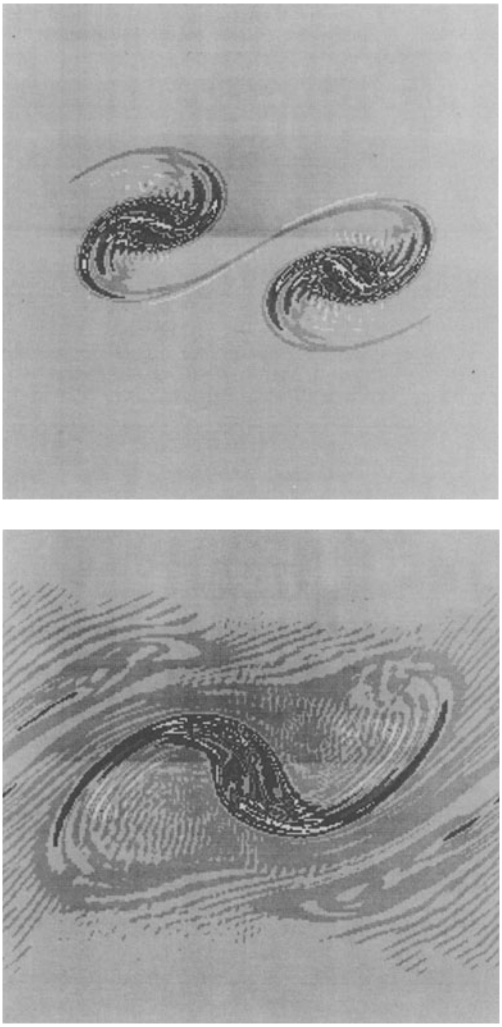

Fig.8. Vorticity contours in a 2D mixing layer (courtesy of P. Comte, Institut Mécanique Grenoble) : (a) before coalescence (b) immediately after coalescence

In Figure 8 we provide the vorticity distribution given by P. Comte which allows a clear visualization of the position of the vortices. From an acoustic point of view the most important characteristic is the velocity component in the direction of propagation, that is to say, component v. Therefore in Figure 9 we give the v distribution in gray levels. The dark gray regions correspond to positive components and the light gray to negative ones.

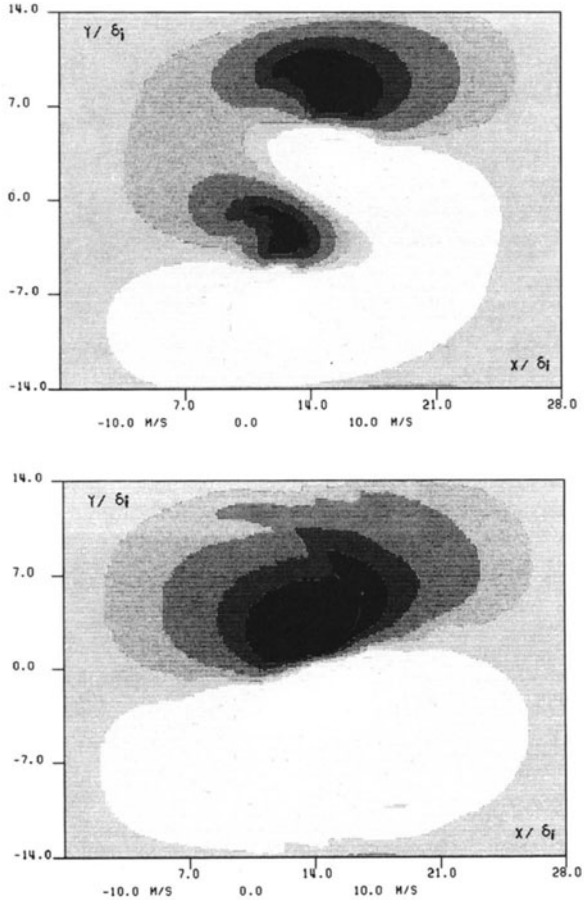

Fig.9. Iso-contours of the lateral velocity v for the flow pictured in Figure 8 : (a) before coalescence (b) immediately after coalescence. Dark gray regions are positive v and light gray regions are negative v

The acoustic fields we obtained using the parabolic equation method are given in Figure 10. The similarity with the maps of Figure 9 is striking. Before coalescence takes place, we see four regions where weakening and strengthening of the acoustic field alternate. These regions correspond to the four high velocity regions of Figure 9. After coalescence, we note a region of strong strengthening and a region of strong weakening associated with regions where the absolute magnitude of v is very large.

Despite the absence of ray tracing, which is difficult here because of the interpolation needed to express the derivatives, it is possible to obtain a qualitative idea of the behavior of an acoustic wave. Indeed, focusing and divergence of rays are essentially linked to the presence of intense velocity gradients between vortices as well as inside the vortices. Illustrations are provided in Figure 11.

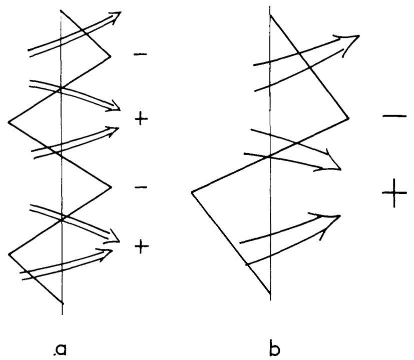

Fig.11. Sketch illustrating the effect of velocity gradients on th propagation of acoustic rays through a 2D mixing layer. (a) before coalescence (b) after coalescence.

This allows us to correctly interpret the visualizations of the acoustic fields. The strongest velocity gradients occur in the case (b) producing focusing and diverging effects which are stronger than in case (a).

5. Conclusion

When applied to individual realizations, the ray theory and the parabolic equation methods can provide complementary and original results. For example, ray paths, caustics, reinforced or weakened zones of the transmitted acoustic field can be clearly visualized.

Averaging over an ensemble of such realizations permit us to obtain statistical results which have been compared with theoretical predictions in the case of 2D isotropic turbulence. For the fluctuations of acoustic intensity, similar results are obtained using both these approaches in the range of weak fluctuations described by the Rytov theory, and in the range of large fluctuations where the saturation phenomenon takes place. In addition, our simulations permits us to cover the intermediate region where no theory is currently available. For the fluctuations of propagation time, which can be interpreted as phase changes or wave front distortions, our numerical results show the limits of the classical approaches (e.g. Chernov) as soon as caustics occur.

The representation of a (vectorial) velocity field by a (scalar) refraction index ($-u'/c_0$ versus $-t'/2.T_0$) also requires special scrutiny. The distribution of kinetic energy among the different scales of the inhomogeneous field has to be taken into account in the r.m.s. level u' as well as in the length scale L used to make a non dimensional representation of the results.

Using the same technique it could be possible to create inhomogeneous and/or random media involving non negligible backscattering due to strong inhomogeneities and to compute the resulting acoustic fields by solving forward and backward parabolic equations.

Aknowledgements

The authors would like to thank R. Lambrecht for her very kind editorial assistance.

References

Blanc-Benon, Ph. and Juvé, D., 1987: Statistical properties of acoustic waves propagating through turbulent thermal fields. *AIAA Paper 87-2727*, AIAA 11th Aeroacoustics Conf., Palo-Alto.

Blanc-Benon, Ph., Juvé, D., Karweit, M. and Comte-Bellot, G., 1990: Simulation numérique de la propagation des ondes acoustiques à travers une turbulence cinématique, *J. d'Acoustique 3*, 1, 1-8.

Blanc-Benon, Ph. and Juvé, D., 1990: Simulation numérique de la propagation d'une onde acoustique dans une turbulence bidimensionnelle par une méthode de rayons. 1er Congrès Français d'Acoustique, *Supplément au Journal de Physique*, Editions de Physique, C2, 1149-1152.

Candel, S.M., 1977: Numerical solution of conservation equations arising in linear wave theory : application to aeroacoustics, *J. Fluid Mech.*, **83**, 465-493.

Candel, S.M., 1979: Numerical solution of wave scattering problems in the parabolic approximation, *J. Fluid Mech.*, **90**, 465-507.

Chernov, L.A., 1960: *Wave propagation in a random medium.* Mc Graw-Hill, New York.

Codona, J.L., Creamer, D.B., Flatte, S.M., Frelich, R.G. and Henyey, F.S., 1985: Average arrival time of wave pulses through continuous random media, *Phys. Rev. Letters 55*, (1), 9-12.

Comte, P., Lesieur, M., Laroche, H. and Normand, X., 1989: Numerical simulations of turbulent plane shear layers - in *Turbulent Shear Flows 6*, Springer-Verlag, 360-380.

Corcos, G.M. and Sherman, F.S. 1984 The mixing layer : deterministic models of a turbulent flow. Part 1. Introduction and the two-dimensional flow, *J. Fluid Mech.*, **139**, 29-65.

DiNapoli, F.R. and Deavenport, R.L., 1979: Numerical models of underwater acoustic propagation. In *Ocean Acoustics*, ed. by J.A. De Santo, Topics in Current Physics, Springer Verlag. 79, 157.

Hesselink, L. and Sturtevant, B., 1988: Propagation of weak shocks through a random medium, *J. Fluid Mech.*, **196**, 513-553.

Ishimaru A., 1978: *Wave propagation and scattering in random media*, Vol. 2. Academic Press.

Keller, J.B., 1962: Wave propagation in random media. Proc. Symp. *Appl. Math. 13*, Amer. Math. Soc. Providence R.I.

Kraichnan, R.H., 1970: Diffusion by a random velocity field, *Phys. Fluids*, 13, 22-31.

Kulkarny, V.A. and White, B.S., 1982: Focusing of waves in turbulent inhomogeneous media, *Phys. Fluids 25*, 10, 1770-1784.

Lesieur, M., Staquet, C., Le Roy, P. and Comte, P., 1988: The mixing layer and its coherence examined from the point of view of two-dimensional turbulence, *J. Fluid Mech.*, **192**, 511-534.

Martin, J.M. and Flatte, S.M., 1988: Intensity images and statistics from numerical simulation of wave propagation in 3-D random media. *Applied Optics 27*, (11), 2111-2126.

Spivack, M. and Uscinski, B.J., 1988: Accurate numerical solution of the fourth-moment equation for very large values of Γ . *J. Modern Optics*, 35, 11, 1741-1755.

Tappert, F.D. 1977: The parabolic approximation method - in *Wave propagation and underwater acoustics*, ed. by J.B. Keller and J.S. Papadakis. Lecture Notes in Physics, Springer-Verlag. 70, 224-287.

Tatarski, V.I. 1971: *The effects of the turbulent atmosphere on wave propagation.* IPST Keter Press, Jerusalem.

Tatarski, V.I. and Zavorotnyi V.U., 1980: Strong fluctuations in light propagation in a randomly inhomogeneous medium. *Progress in Optics*, edited by E. Wolf, Vol. 18, North Holland, New York .

White, B.S., 1984: The stochastic caustic. *SIAM J. Appl. Math. 44*, 1, 127-149.